The Angiostatic Protein 16K Human Prolactin Significantly Prevents Tumor-Induced Lymphangiogenesis by Affecting Lymphatic Endothelial Cells

Virginie Kinet,* Karolien Castermans,* Stéphanie Herkenne, Catherine Maillard, Silvia Blacher, Michelle Lion, Agnès Noël, Joseph A. Martial, and Ingrid Struman

Groupe Interdisciplinaire de Génoprotéomique Appliquée (GIGA) Research (V.K., K.C., S.H., M.L., J.A.M., I.S.), Molecular Biology and Genetic Engineering Unit, and GIGA Cancer (C.M., S.B., A.N.), Tumor and Development Biology Unit, University of Liège, 4000 Liège, Belgium

The 16-kDa angiostatic N-terminal fragment of human prolactin (16K hPRL) has been reported to be a new potent anticancer compound. This protein has already proven its efficiency in several mouse tumor models in which it prevented tumor-induced angiogenesis and delayed tumor growth. In addition to angiogenesis, tumors also stimulate the formation of lymphatic vessels, which contribute to tumor cell dissemination and metastasis. However, the role of 16K hPRL in tumor-induced lymphangiogenesis has never been investigated. We establish *in vitro* that 16K hPRL induces apoptosis and inhibits proliferation, migration, and tube formation of human dermal lymphatic microvascular endothelial cells. In addition, in a B16F10 melanoma mouse model, we found a decreased number of lymphatic vessels in the primary tumor and in the sentinel lymph nodes after 16K hPRL treatment. This decrease is accompanied by a significant diminished expression of lymphangiogenic markers in primary tumors and sentinel lymph nodes as determined by quantitative RT-PCR. These results suggest, for the first time, that 16K hPRL is a lymphangiostatic as well as an angiostatic agent with antitumor properties. **(*Endocrinology* 152: 4062–4071, 2011)**

The 16-kDa N-terminal fragment of human prolactin, 16K human prolactin (16K hPRL), has been identified as a potent angiostatic compound (1–5). This prolactin variant is generated from full-length prolactin by cathepsin-D mediated cleavage (6). In contrast to full-length prolactin, 16K hPRL inhibits proliferation and migration of vascular endothelial cells and induces vascular endothelial cell cycle arrest and apoptosis (2–5, 7–10). This angiostatic activity of 16K hPRL appears to be mediated by a currently unreported saturable high-affinity binding site distinct from the prolactin (PRL) receptor (11). The physiological relevance of 16K hPRL has recently been described by Hilfiker-Kleiner *et al.* (12) in postpartum cardiomyopathy. In this disease, high local levels of 16K hPRL impair the cardiac capillary network, which contributes to heart failure. In addition, urine, serum, and amniotic fluid of women with severe preeclampsia compared with healthy pregnant women contained increased amounts of 16K hPRL.

These data suggest that 16K hPRL contributes to the endothelial cell dysfunction and compromised birth weight associated with this disease (13). Erdmann *et al.* (14) demonstrated the presence of bovine 16K PRL in the corpus luteum. This bioactive fragment of prolactin was able to affect corpus luteum-derived endothelial cells and might therefore contribute to the corpus luteum regression mechanism. Due to its negative effects on angiogenesis, 16K hPRL is a potent anticancer compound (15). This

ISSN Print 0013-7227 ISSN Online 1945-7170
Printed in U.S.A.

doi: 10.1210/en.2011-1081 Received April 6, 2011. Accepted July 29, 2011.
First Published Online August 23, 2011

* V.K. and K.C. contributed equally to the study.

Abbreviations: bFGF, Basic fibroblast growth factor; eGFP, enhanced green fluorescent protein; FBS, fetal bovine serum; HMVECdLy, human dermal lymphatic microvascular endothelial cell; 16K hPRL, 16K human PRL; PAI-1, plasminogen activator inhibitor; PPIA, cyclophilin A; PRL, prolactin; qRT-PCR, quantitative real time-PCR; SLN, sentinel lymph node; TRP, Tyrosinase-related protein 1; VEGF, vascular endothelial growth factor; VEGFR, VEGF receptor.

protein inhibits capillary endothelial cell outgrowth induced by basic fibroblast growth factor (bFGF) and/or vascular endothelial growth factor (VEGF), two major angiogenic growth factors released by tumor cells. In addition, 16K hPRL, produced by human HCT116 colon cancer cells, reduces their ability to form subcutaneous tumors in $Rag^{-/-}$ mice (16). Furthermore, Kim *et al.* (17) demonstrated that adenovirus-mediated 16K hPRL expression by prostate cancer cells decreases tumor growth. Studies in our laboratory on the B16F10 mouse melanoma tumor model showed a significant tumor growth delay after 16K hPRL treatment and distinct tumor vasculature characterized by small and narrow vessels (18, 19). Additionally, Nguyen *et al.* (19) demonstrated in an experimental lung metastasis model via iv injection of B16F10 melanoma cells without the development of a primary tumor that 16K hPRL treatment of mice before intravenous tumor inoculation decreased tumor metastasis in the lungs.

Besides angiogenesis, the outgrowth of lymphatic vasculature, *i.e.* lymphangiogenesis, is also stimulated by VEGF family members released by tumor cells during tumor development (20). Lymphangiogenesis is a complex process comprising multiple events, including lymphatic endothelial cell proliferation, migration, organization, and vessel maturation (21). The lymphatic vasculature is essential for the maintenance of interstitial tissue fluid, immune function, and absorption of dietary fats. Tumor-associated lymphangiogenesis has potential significance not only at the primary tumor site but also in the sentinel lymph nodes (SLN), the first set of nodes to receive drainage from the primary tumor (22, 23). The distinct structural features of lymphatic vessels, *e.g.* permeability and absence of basement membrane, make them more accessible to tumor cells than blood vessels and facilitate tumor cell dissemination and metastasis (21, 24). The extent of lymph node involvement is the most important indicator of tumor aggressiveness (21, 24–26).

Our hypothesis was that angiostatic protein 16K hPRL disrupts not only tumor-induced angiogenesis but also lymphangiogenesis, making it a strong anticancer compound. We demonstrate here *in vitro* that 16K hPRL is able to counteract the multiple events that lead to new lymphatic vasculature. Similar to blood endothelial cells, 16K hPRL reduces lymphatic endothelial cell proliferation, migration, and tube formation and induces cell apoptosis. Additionally, B16F10 tumor-bearing mice show a modest lymphatic network in the primary tumor and in the SLN after 16K hPRL treatment compared with controls as determined by immunohistochemical and quantitative RT-PCR analysis of numerous lymphatic markers.

Materials and Methods

Cell culture

Primary neonatal human dermal lymphatic microvascular endothelial cells (HMVECdLy) derived from a single donor were purchased from Lonza (Verviers, Belgium). They were maintained in EGM2-MV medium (Lonza) containing endothelial cell growth supplements provided by the supplier. Due to their primary condition, HMVECdLy were used for a maximum of six passages.

B16F10 mouse melanoma cells were obtained from the American Type Culture Collection (ATCC CRL-6475, Manassas, VA) and cultured in DMEM 4500 supplemented with 10% fetal bovine serum (FBS), 100 U/ml penicillin, and 100 μg/ml streptomycin. All cells were incubated at 37 C in a 5% CO_2 humid atmosphere. All culture reagents were purchased from Invitrogen (Carlsbad, CA).

B16F10 transfection

B16F10 cells were transfected with a plasmid that expresses enhanced green fluorescent protein (eGFP) and puromycin resistance (pIRESpuroeGFP) using Lipofectamine PLUS at a ratio of 1:1 according to the manufacturer's instructions (Invitrogen, Carlsbad, CA). Transfected cells were selected with puromycin at a final concentration of 1 μg/ml, and several colonies were picked out and expanded for analysis. Colonies displaying the highest level of eGFP expression were selected (Supplemental Fig. 1, published on The Endocrine Society's Journals Online web site at http://jcem.endojournals.org).

Recombinant adenovirus vector construction

16K-Ad is a defective recombinant E1-E3-deleted adenovirus vector encoding a secreted peptide consisting of the first 139 amino acids of PRL. This adenovirus vector was constructed as described by Nguyen *et al.* (19) and Pan *et al.* (27), using the Adeno-X expression system (BD Biosciences, Erembodegem, Belgium). Purification and titration of the recombinant adenoviruses were performed, respectively, with the BD Adeno-X virus purification kit and the Adeno-X rapid titer kit (BD Biosciences), according to the manufacturer's instructions. Null-Ad is a control adenovirus carrying an empty expression cassette.

Animals and tumor model

Female C57BL/6J mice (n = 40) obtained from the Central Animal Facility of Centre Hospitalier Univesitaire Liège (Liège, Belgium) were inoculated with 2×10^5 eGFP-B16F10 cells in 20 μl PBS by sc injection into the right hind footpad. Two days before tumor inoculation, mice were treated by iv injection with 10^9 pfu adenovirus carrying 16K hPRL or an empty expression cassette. This treatment was repeated 1 wk after the first iv injection. Primary tumors became visible 9 d after tumor injection. Tumor growth was assessed by measuring the length and width of each tumor every 1 or 2 d using calipers. Tumor volume was calculated by the formula: length $\times$ width^2 $\times$ 0.5. Mice were euthanized and tissues harvested either 1 or 2 wk after tumor inoculation.

All experiments were approved by the Institutional Ethical Review Committee for Animal Experiments of the University of Liège.

Western blot analysis

Cyclin D1 protein expression

Cytoplasmic cell lysate (20 μg) was resolved by SDS-PAGE (12%), and the bands were transferred to a polyvinylidene fluoride membrane (Millipore Corp., Bedford, MA). The blots were blocked for 1 h with 8% milk in Tris-buffered saline with 0.1% Tween 20 and probed for 1 h with primary antibodies: anticyclin D1 (sc-718; Santa Cruz Biotechnology, Inc., Santa Cruz, CA) and anti-tubulin (ab6046; Abcam, Cambridge, UK). After three washes with Tris-buffered saline with 0.2% Tween 20, antigen-antibody complexes were detected by means of peroxidase-conjugated secondary antibody and an enhanced fluorochemiluminescent system (ECL-plus; Amersham Biosciences, Arlington Heights, IL).

16K hPRL in mouse serum

One microliter of serum from mice treated by null-adenoviruses or 16K adenoviruses was resolved by SDS-PAGE (12%) and transferred to a polyvinylidene fluoride membrane (Millipore). Membranes were saturated overnight with 8% milk in Tris-buffered saline with 0.1% Tween 20 followed by incubation for 1 h with polyclonal rabbit anti-hPRL antibody (A0569; Dako, Glostrup, Denmark) and for 1 h with peroxidase-conjugated goat antirabbit antibody (7074; Cell Signaling Technology, Beverly, MA). 16K hPRL detection was carried out by chemiluminescence using the ECL Plus kit (Amersham Biosciences).

Quantitative real time-PCR (qRT-PCR)

Total RNA from tissues was isolated using the QIAGEN Rneasy minikit (QIAGEN, Hilden, Germany) and reverse transcribed with the iScript cDNA synthesis kit (Bio-Rad Laboratories, Nazareth Eke, Belgium) according to the manufacturer's instructions. The resulting cDNA was used for real-time PCR with SYBR mastermix (Diagenode, Liège, Belgium). Thermal cycling was performed on an Applied Biosystems 7000 detection system (Applied Biosystems, Foster City, CA). The relative expression was calculated using the formula $2^{-\Delta\Delta CT}$ using cyclophilin A (PPIA) or β-2-microglobulin as the internal control. Primer sequences are available upon request.

Immunohistochemical staining

Tissues from the B16F10 model were fixed in 4% paraformaldehyde for 2 h, immersed in sucrose, and rinsed with PBS before being snap frozen. After blocking endogenous peroxidase, tissue sections (6 μm) were immersed in 20% fetal calf serum in PBS 1% BSA 0.1% Tween 20 to prevent a specific staining and were incubated in rat antimouse CD31 (557355; BD Biosciences Pharmingen, Franklin Lakes, MA) or rabbit polyclonal anti-Lyve-1 (70R-LR005; Fitzgerald Industries International, North Action, MA) followed by incubation with a biotinylated secondary antibody (E0432; goat antirabbit biotin; Dako, Glostrup, Denmark, and 712-065-150; donkey antirat biotin; Jackson ImmunoResearch, Suffolk, UK) and the streptABComplex/HRP complex. Staining was revealed using 3-amino-9-ethylcarbazole + substrate chromogen. Sections were finally counterstained with hematoxylin and mounted with Glycergel (all Dako).

Image processing and measurements

Total tumor and lymph node sections were scanned using an Olympus AX-Macro research system microscope (Olympus, Aartselaar, Belgium). Image processing and measurements were performed with the Aphelion 3.2 software from Adsis (Hérouville, France) on a personal computer as described previously (18, 19). Briefly, complete tumor and lymph node sections were analyzed for each condition. Immunostaining for CD31 and Lyve-1 of histological tissue sections were used to distinguish respectively blood and lymphatic vessels from tissue. They appear in red in the red-green-blue color image. The red component was first extracted and the resulting image was further processed as follows: 1) vessels were segmented automatically using the endotropy of the histogram of gray-level intensities; 2) an erosion morphological filter was applied to eliminate small artifacts; 3) because this last operation reduces the size of the vessels, a geodesic dilation was carried out to make them recover their real sizes; 4) all vessels touching the border of the image were eliminated; and 5) to identify and measure the area of each vessel, the vessels were labeled with different colors.

The following measurements were performed: 1) vessel number was the number of vessels per unit of tissue area; 2) vessel area was mean area occupied by one vessel (vessel size); and 3) vessel area density was the percentage of tissue area occupied by vessels.

Production of recombinant proteins

Recombinant 16K hPRL was produced and purified from *Escherichia coli* as previously described (5). The purity of the recombinant protein exceeded 95% (as estimated by Coomassie blue staining), and the endotoxin level was 0.5 pg/ng recombinant protein, as quantified by the Rapid Endo Test of the European Endotoxin Testing Service (Lonza, Verviers, Belgium). For all *in vitro* experiments, a control for endotoxin was used. However, we did not observe any effect with this control.

Apoptosis assay

HMVECdLy were plated in 96-well culture plates at a density of 5000 cells per well and allowed to attach in EGM2-MV (Lonza). Next, cells were incubated overnight in EBM2 containing 0.5% of FBS followed by the addition of 100 nM of 16K hPRL. Apoptosis was analyzed 8 h later by measuring the caspase-3/7 activity with the Caspase-Glo 3/7 assay (Promega Corp., Madison, WI) according to the manufacturer's instructions.

Proliferation assay

HMVECdLy were plated in 96-well culture plates at a density of 4000 cells per well in EGM2-MV (Lonza) and allowed to adhere for 24 h. Complete medium was then removed and replaced by EBM2 containing 2% FBS, 0.1% epithelial growth factor, 0.04% hydrocortisone, and 0.1% gentamicin/amphotericin B. Cells were treated with 100 nM of 16K hPRL and proliferation was analyzed 72 h later using the colorimetric cell proliferation reagent WST-1 kit (Roche, Mannheim, Germany).

Tube formation assay

HMVECdLy were plated in 48-well culture plates coated with a film of collagen at a density of 50,000 cells/well in EGM2-MV (Lonza). When the cells formed a confluent mono-

layer, they were covered with 150 μl of collagen (28). After 2 h at 37 C, the cells were treated with the different agents diluted in EBM2 containing 2% FBS. Sixteen hours later, the cells were incubated with calcein-AM (2 μM; Sigma-Aldrich, Bornem, Belgium) for 20 min. Quantitative analysis of the network structure was performed by measuring all tube lengths using ImageJ (http://rsbweb.nih.gov/ij/) and adding these measurements to obtain a total tube length per condition. For each condition five photos were analyzed in three independent experiments.

Migration assay

Boyden chamber assay

Migration of HMVECdLy was determined using a Boyden chamber (8 μm pore size; Corning Inc., Corning, NY). Fifty thousand HMVECdLy were seeded in EBM2 containing 5% FBS, 0.1% epithelial growth factor, 0.04% hydrocortisone, and 0.1% gentamicin/amphotericin B in the upper chamber previously coated with gelatin 0.005%. VEGF-C (320 μM) was added as chemoattractant to the lower chamber. After 24 h, cells in the upper chamber were carefully removed using cotton buds and cells at the bottom of the membrane were fixed and stained with 4% Giemsa. Quantification was performed on by counting the stained cells on the membrane. For each condition five photos were analyzed in three independent experiments.

Wound assay

Fifty thousand HMVECdLy were cultured to a confluent cell monolayer in EGM2-MV (Lonza) in 48-well culture plates. Using a sterile 20-μl pipette tip, a wound was made in the well. The wounded monolayers were washed with free medium to remove nonadherent cells.Next, cells were treated with the different compounds for 8 h in EBM2 containing 5% FBS, 0.1% endothelial growth factor, 0.04% hydrocortisone, and 0.1% gentamicin/amphotericin B. The plate was placed under a phase-contrast microscope and images were acquired according to fixed reference points to allow the same fields during the image acquisition. The width of the wound was determined at time zero and 8 h after onset of the experiment. The rate of cell migration is inversely correlated to the wound width. For each condition five photos were analyzed in three independent experiments.

In vivo Matrigel plug assay

Adult female C57BL/6J mice (6–8 wk of age) were sc injected with 500 μl of growth factor-reduced Matrigel (Becton Dickinson, Bedford, MA) containing 640 μM of VEGF-C (R&D Systems, Oxon, UK) or with Matrigel containing 640 μM of VEGF-C and 200 nM of 16K hPRL. After 9 d, injected Matrigels were isolated and were snap frozen.

Statistical analysis

All data are expressed as means ± SEM. Statistical analyses (Mann-Whitney test) were carried out with the Prism 5.0 software (GraphPad Software, La Jolla, CA). Statistical significance was set at $P < 0.05$.

Results

16K hPRL inhibits proliferation and tube formation and induces apoptosis of lymphatic endothelial cells

To establish its putative lymphangiostatic potential, we first tested the efficacy of 16K hPRL on endothelial cells derived from lymphatic vessels. We used HMVECdLy as previously described (29, 30). The cells were positive for Podoplanin, Lyve-1 and VEGF receptor (VEGFR)-3 (data not shown) and were accordingly sensitive to VEGF-C by showing increased proliferation when treated with this growth factor (Fig. 1A). This proliferation induction was reduced upon treatment with 100 nM of 16K hPRL (Fig. 1A). In addition, we analyzed the level of cyclin D1, a factor important in the cell transition from G_1 into S. This factor is decreased in blood endothelial cells after 16K hPRL treatment (4). Treatment of 72 h with 16K hPRL showed a dose-dependent decrease in cyclin D1 expression in HMVECdLy (Fig. 1B).

Next, we studied the effect of 16K hPRL on capillary organization of HMVECdLy between two collagen layers. Although a treatment with 320 μM of VEGF-C increased the capillary tube formation, 16K hPRL prevented this augmentation (Fig. 1C). 16K hPRL is known to induce apoptosis in blood endothelial cells by inducing caspase-3/7 activity. Indeed, in the present study, serum starved HMVECdLy also showed increased apoptosis after treatment with 100 nM of 16K hPRL, as demonstrated by the augmented activity of caspase-3/7 (Fig. 1D).

We also tested full-length prolactin on lymphatic endothelial cell proliferation and apoptosis but did not detect any effect (data not shown).

16K hPRL inhibits lymphatic endothelial cell migration *in vitro* and *in vivo*

During lymphangiogenesis, lymphatic endothelial cells migrate toward a positive stimulus and form tubes by interconnection. This process was investigated in two different *in vitro* assays. In a Boyden chamber assay, HMVECdLy migration was strongly increased toward the chemoattractant VEGF-C, as shown in Fig. 2A. Treatment of the cells with 16K hPRL significantly repressed the migration toward VEGF-C (Fig. 2A).

The *in vitro* wound assay is particularly suitable for studying the importance of cell-matrix and cell-cell interactions during cell migration (31). Stimulation of the HMVECdLy with VEGF-C induced cell migration, and treatment of the cells with 16K hPRL blocked this induction completely (Fig. 2B). Furthermore, even in nonstimulated cells, we observed an inhibition of cell migration after 16K hPRL treatment (Fig. 2B).

The antimigrative effect of 16K hPRL observed *in vitro* was confirmed *in vivo* through a Matrigel plug assay in mice. Analysis of the VEGF-C enriched Matrigel, which was isolated 9 d after sc injection in mice, revealed lymphatic cell recruitment. Quantification of several lymphatic markers by qRT-PCR demonstrated expression of *Podoplanin*, *VEGFR-3*, and *Lyve-1* in these Matrigels.

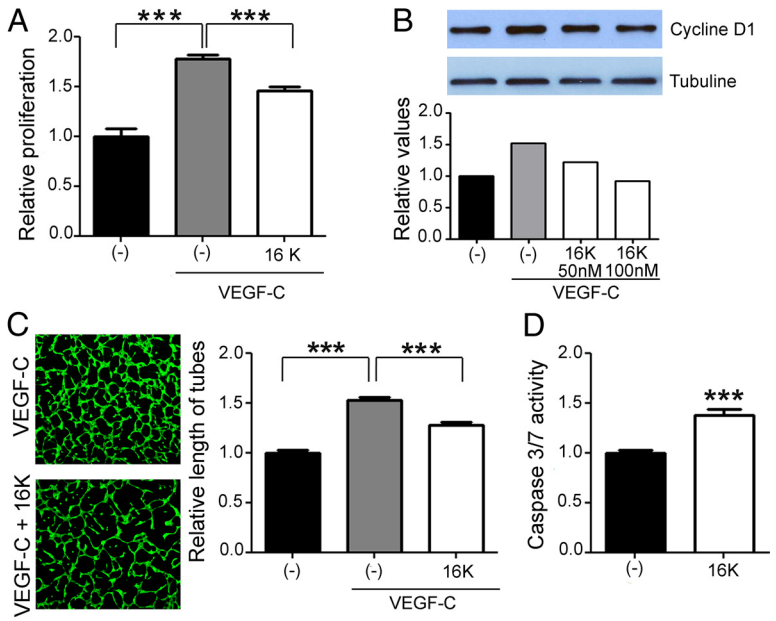

FIG. 1. 16K hPRL inhibits proliferation and tube formation and induces apoptosis of HMVECdLy. A, 16K hPRL decreases proliferation of HMVECdLy cultured in medium containing 2% FBS as determined by the colorimetric WST-1 test after 72 h of treatment with 100 nM 16K hPRL (*black bar*, control; *gray bar*, +320 μM VEGFC; *white bar*, +320 μM VEGFC + 100 nM 16K hPRL). B, 16K hPRL decreases dose-dependently the protein levels of cyclin D1 as determined by Western blot analysis (*top panels*). Differences in protein expression were analyzed using ImageJ (National Institutes of Health) and normalized to tubulin expression. The result is representative of two similar and independent experiments. C, 16K hPRL decreases tubulogenesis of HMVECdLy cultured in medium containing 2% FBS. Cells were seeded between two layers of collagen and treated for 16 h. Living cells were stained with calcein-AM. Analysis of the capillary network was performed by measuring the total length of tubes (*black bar*, control; *gray bar*, +320 μM VEGF-C; *white bar*, +320 μM VEGF-C + 100 nM 16K hPRL). D, 16K hPRL increases caspase-3/7 activity of serum-starved (0.5% FBS) HMVECdLy. Caspase-3/7 activity of HMVECdLy was measured after a treatment of 8 h with 100 nM of 16K hPRL (*black bar*, control; *white bar*, +100 nM 16K hPRL) The results are presented as means ± SEM of at least three independent experiments. For each test, the control sample was arbitrarily fixed at 1. ***, $P < 0.0005$.

The mRNA expression level of *Podoplanin* was significantly reduced when VEGF-C-enriched Matrigel contained 16K hPRL. The gene transcripts of *VEGFR-3* and *Lyve-1* showed the same trend although statistical significance was not reached. These results suggest a reduced recruitment and migration of lymphatic cells into the Matrigel (Fig. 2C).

All these results strongly suggest an inhibitory effect of 16K hPRL on lymphatic endothelial cell migration.

In vivo tumor-induced lymphangiogenesis in a mouse eGFP-B16F10 footpad melanoma model

The mouse eGFP-B16F10 footpad melanoma model was used to investigate tumor-induced lymphangiogenesis. This model entails the sc injection of eGFP-B16F10 mouse melanoma cells into the right hind footpad of C57BL/6J mice. The lymphatic system of the foot drains directly through the popliteal lymph node. Therefore, primary eGFP-B16F10 footpad tumors are likely to induce lymphangiogenesis and metastasis in the popliteal lymph node. An advantage of this model is reduced experimental heterogeneity due to the anatomic, constant and superficial location of the single popliteal lymph node (32–34). The popliteal lymph node is called the SLN from now on.

Before injection, B16F10 cells were transduced with a plasmid vector encoding the eGFP gene. The eGFP-expressing tumor cells can be easily visualized by fluorescent microscopy allowing assessment of metastasis in the sentinel lymph node. The eGFP-transduced B16F10 cells showed the same growth curves as wild-type B16F10 cells (Supplemental Fig. 1, A and B). A pilot study confirmed that, in this model, the formation of an eGFP-B16F10 primary tumor in the footpad of mice induced the development of the lymphatic vasculature in the draining sentinel lymph node. We analyzed the expression of lymphatic markers in the SLN and in the nontumor-draining contralateral lymph node by qRT-PCR 14 d after tumor inoculation in the right hind footpad. The SLN showed significantly increased relative expression levels of *Lyve-1* and *VEGFR-3* compared with the nontumor-draining contralateral lymph node (Fig. 3A).

16K hPRL delays tumor growth and impedes neovascularization in the mouse eGFP-B16F10 footpad melanoma model

Because 16K hPRL had not yet been used in this footpad B16F10 tumor model, we first established its antitumor effects. Mice treated with adenoviruses encoding 16K hPRL (16K-Ad) showed a significant delay in tumor growth compared with mice treated with control adenoviruses (Null-Ad) (Fig. 3B). Analysis by Western blot of serum from the treated mice confirmed the presence of 16K hPRL protein levels throughout the experiment (Fig. 3C). A band running higher than that seen for recombinant 16K hPRL produced in *E. coli* was observed. This is due to the N-glycosylation of Asn 31 of 16K hPRL as previously shown and does not affect the biological activity of 16K hPRL (19, 27). Next, we determined the angiostatic potential of 16K-Ad treatment by scrutinizing the tumor vasculature. We found that the number of tumor blood vessels was slightly although not significantly reduced by 16K-Ad treatment (Fig. 3D). However, tumor

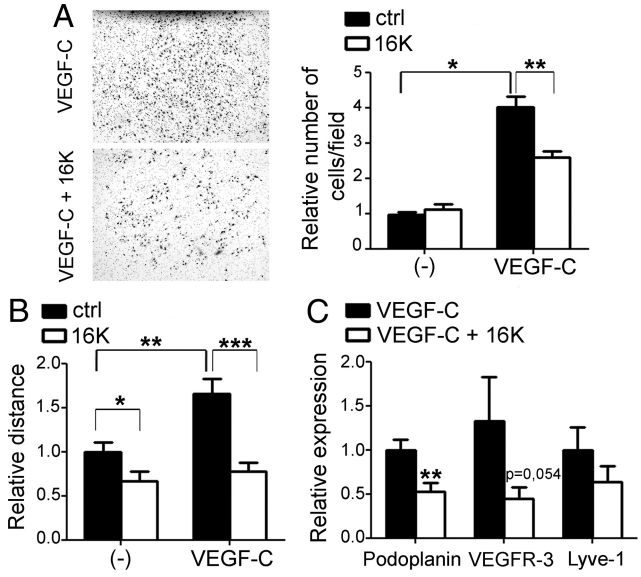

FIG. 2. 16K hPRL impairs lymphatic endothelial cell migration. A, Boyden chamber assay. HMVECdLy cells were cultured in medium containing 5% FBS. Cell migration was measured after 24 h by counting the cells on the membrane. *Left panel*, Representative images of membranes containing migrated cells (*black dots*) after treatment or not with 16K PRL, *Right pane*l, Quantification of cell migration through the membrane. B, Wound assay. HMVECdLy cells were cultured in medium containing 5% FBS. Distance of cell migration was measured after 8 h. The results are presented as means ± SEM of at least four independent experiments. C, Matrigel invasion assay. 16K hPRL down-regulates expression of lymphatic markers (Podoplanin, VEGFR-3, Lyve-1) in Matrigel. RNA was extracted from Matrigel containing 640 μM VEGF-C (n = 9) or 640 μM VEGF-C + 16K hPRL (n = 10) derived from mice (two independent experiments). Transcript levels were analyzed by qRT-PCR and normalized to PPIA. The results are presented as relative expression values ± SEM. For each test, and the control sample was arbitrarily fixed at 1. *, $P < 0.05$; **, $P < 0.01$; ***, $P < 0.0005$.

blood vessels of 16K-Ad treated mice appeared smaller and collapsed compared with Null-Ad treated mice. As expected, computer-assisted image analysis revealed that the total blood vessel area density and the average blood vessel area were 65 and 66% lower in the 16K-Ad-treated mice, respectively, than in the Null-Ad mice (Fig. 3D). These results are in line with our previous publications in which we used B16F10 tumor cells in a sc flank model. 16K hPRL treatment reduced blood vessel area and decreased the vessel number, which combined lead to globally reduced vessel density (18, 19).

16K hPRL inhibits lymphangiogenesis in the primary tumor and the sentinel lymph node

Next, we determined the number of lymphatic vessels within the primary tumor. Few lymphatic vessels were present in the primary tumor. This is in line with previous studies demonstrating that melanoma growth does not obviously alter the sparse lymphatic vasculature in the footpads and that only few lymphatic vessels are present in the primary tumor (32). However, we were able to observe a small decrease in the number of lymphatic vessels and the total vessel area density when mice were treated with 16K-Ad, indicating that 16K hPRL might have an inhibitory effect on tumor induced lymphangiogenesis (Fig. 4A). Additionally, we determined decreased expression levels of lymphangiogenic markers, which were significant for *Prox-1* in primary tumor tissues of 16K-Ad treated mice compared with Null-Ad-treated mice (Fig. 4B).

Next, we analyzed the lymphatic network in the sentinel lymph nodes of tumor-bearing mice by immunohistochemical staining of tissue sections with Lyve-1. Fourteen days after tumor injection, we observed a significant inhibition of tumor-induced lymphangiogenesis by 16K-Ad in the sentinel lymph nodes. This was characterized by a decrease in the total vessel area, which was occupied by narrow lymphatic vessels (Fig. 4C). The number of lymphatic vessels was not attenuated. In addition, we detected a significant decrease in the mRNA expression levels of *Lyve-1*, *VEGFR-3*, *Prox-1*, and *Podoplanin* in 16K-Ad-treated mice compared with Null-Ad mice (Fig. 4D).

16K hPRL does not affect the establishment of metastasis in the lymph nodes

We assessed by immunofluorescent microscopy that 50% of the Null-Ad-treated mice possessed eGFP-positive B16F10 metastatic lesions in their SLN 14 d after tumor inoculation. Surprisingly, we also detected eGFP-B16F10 metastatic lesions in 40% of 16K-Ad-treated mice. Because these results are in high contrast with the study of Nguyen *et al.* (19), who did show an inhibition of metastasis in an iv experimental B16F10 model, we monitored B16F10 metastasis by expression analysis of Tyrosinase-related protein-1 (*TRP*) in the current footpad model. *TRP* is a melanocyte-specific marker and therefore a specific marker for B16F10 melanoma (33). Analysis of expression of *TRP* transcripts is a more sensitive detection method compared with eGFP fluorescence to determine tumor dissemination. At 72 h and even earlier at 48 h after tumor inoculation in the right hind footpad, we already detected *TRP* mRNA expression in the foot draining lymph node (data not shown). This suggests that inoculated tumor cells are able to penetrate lymphatic vasculature at the time of injection. This event had not previously been described for this model. Our results imply that this model is not the one of choice for spontaneous tumor metastasis studies.

Discussion

Using complementary *in vitro* and *in vivo* studies designed to clearly delineate the contributing processes of lymphatic

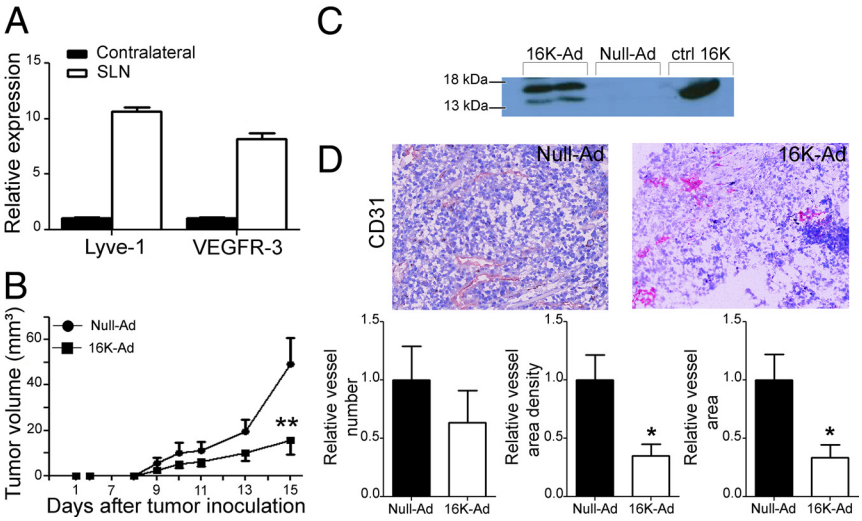

FIG. 3. 16K hPRL delays tumor growth and impedes angiogenesis in eGFP-B16F10 footpad melanoma. A, Relative expression of Lyve-1 and VEGFR-3 mRNA in SLN and contralateral lymph nodes of nontreated tumor bearing mice (n = 5) determined by qRT-PCR. Values were normalized to PPIA. B, Tumor growth curve. C57BL/6J mice were iv inoculated with 10^9 pfu Null-Ad or 16K-Ad at d 1 and 8. eGFP-B16F10 tumor cells were sc injected in the right hind footpad at d 3. Values are mean tumor volume ± SEM (n = 8). C, Western blot of 16K hPRL in serum from mice inoculated with Null-Ad or 16K-Ad. Thirty nanograms of recombinant 16K hPRL were loaded as a control. D, Primary tumors from Null-Ad and 16K-Ad inoculated mice were analyzed for number of vessels, total blood vessel density, and average blood vessel area (CD31 staining, original magnification, ×100). *Columns*, mean; *bars*, SEM. *, $P < 0.05$; **, $P < 0.01$.

growth, we established that the antitumor compound 16K hPRL significantly disrupts lymphangiogenesis particularly in metastatic lesions.

Similar to what we found previously on cultured blood endothelial cells (2–4, 8, 35), we observed an induction of apoptosis and a decrease in proliferation, tube formation, and migration of well-characterized lymphatic endothelial cells after 16K hPRL treatment. In addition, *in vivo* mouse studies suggest an inhibitory effect of 16K-Ad treatment on tumor-induced lymphangiogenesis. The previous results together with our newly generated data lead us to propose that 16K hPRL possesses lymphangiostatic characteristics in addition to its angiostatic properties. It is not a common feature of angiostatic agents to also possess lymphangiostatic properties. Although it seems obvious that multityrosine kinase inhibitors (block VEGFR-1, -2, -3) would target both processes, we found some divergences in the literature. Multikinase inhibitor E7080 has been found to be able to inhibit lymphangiogenesis and lymph node metastasis (36). Surprisingly, for the VEGFR tyrosine kinase inhibitor PTK787/ZK222584, Sini *et al.* (37) demonstrated a lymphangiostatic effect, whereas Schomber *et al.* (38)failed to do so. In addition, endogenous inhibitors (angiostatin, endostatin, and vasohibin-1) have been shown to exhibit lymphangiostatic features (39–42), whereas by contrast, thrombospondin-1 has not (43).

We can only speculate on the mechanism involved in the lymphangiostatic properties of 16K hPRL. The angiostatic activity of 16K hPRL appears to be mediated by an unreported, specific, saturable, high-affinity binding site distinct from the PRL receptor (11). Activation of multiple pathways appears to be the rule rather than the exception with ligands acting on endothelial cells (2). 16K hPRL inhibits bFGF- and VEGF-A-induced endothelial cell proliferation (8, 9). The actions of both bFGF and VEGF-A are regulated by receptors of the tyrosine kinase family, which activate the MAPK pathway. 16K hPRL interferes in the MAPK pathway by blocking Ras in blood endothelial cells (7). Additionally, reduced endothelial cell migration by 16K hPRL treatment is due to downregulation of the Ras-Tiam1-Rac1-Pak1 pathway (10). VEGF-C and VEGF-D act through VEGFR-3, another family member of the tyrosine kinases, which induces MAPK signaling and Ras activation (44). Therefore, 16K hPRL might exert its inhibitory properties on lymphatic endothelial cells via this route. However, preliminary data indicate that 16K hPRL treatment might not effect MAPK activation in HMVECdLy (Herkenne, S, unpublished data). VEGFR-3 signaling also leads to downstream activation of the AKT pathway, which has been associated with lymphatic endothelial cell survival and migration. Current studies in our laboratory suggest an implication of this pathway in the downstream signaling of 16K hPRL in blood endothelial cells (Herkenne, S, unpublished data). The possible inhibition of this pathway by 16K hPRL in HMVECdLy might explain the different effects seen in the proliferation/apoptosis *in vitro* assays and cell migration assays, in which inhibitory effects were more pronounced.

Apoptosis induction by 16K hPRL occurs via the caspase-8- and caspase-9-mediated apoptosis cascades initiated by nuclear factor-κB activation in blood endothelial cells (2, 5). This, however, seems unlikely to be the case in lymphatic endothelial cells. Preliminary studies performed by our laboratory suggest that treatment of the HMVECdLy by 16K hPRL does not induce caspase-8 or -9 activation (data not shown). These preliminary results indicate that 16K hPRL might act differently on blood and lymphatic endothelial cells.

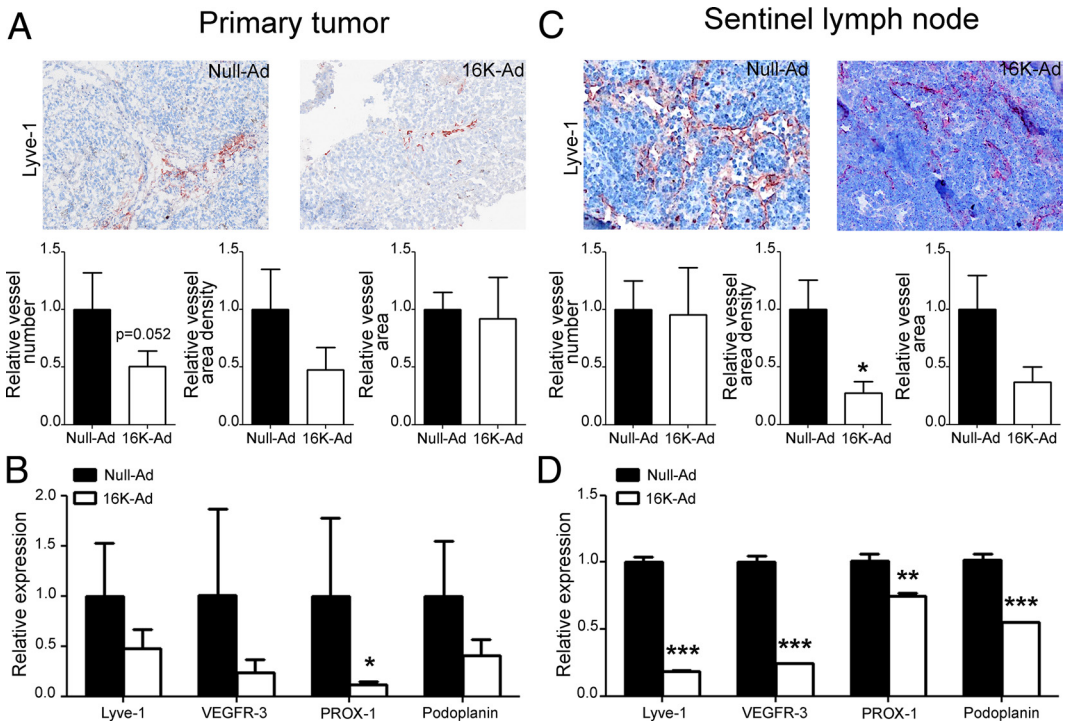

FIG. 4. 16K hPRL inhibits lymphangiogenesis in the primary tumor and the sentinel lymph node A, Primary tumors from Null-Ad- and 16K-Ad-inoculated mice were analyzed for number of vessels, total lymphatic vessel density, and average lymphatic vessel area (Lyve-1 staining, original magnification, ×100). B, Relative mRNA expression of lymphatic markers in primary tumor treated with Null-Ad or16K-Ad determined by qRT-PCR. C, SLN from Null-Ad- and 16K-Ad-inoculated mice were analyzed for number of vessels, total lymphatic vessel density, and average lymphatic vessel area (Lyve-1 staining, original magnification, ×100). D, Relative mRNA expression of lymphatic markers in primary tumor treated with Null-Ad or16K-Ad determined by qRT-PCR. Values were normalized to PPIA. *Columns*, mean; *bars*, SEM. *, $P < 0.05$; **, $P < 0.005$; ***, $P < 0.0005$.

16K hPRL has been demonstrated to inhibit angiogenesis by attenuating the production of nitric oxide and antagonizing the activation of VEGF-inducible endothelial nitric oxide synthase (45, 46). Interestingly, Lahdenranta *et al.* (47) have recently established the role of nitric oxide synthase and nitric oxide in lymphangiogenesis and lymphatic metastasis. Because 16K hPRL represses nitric oxide synthase and nitric oxide expression, this might partly explain the simultaneous inhibition of tumor-associated angiogenesis and lymphangiogenesis as well as metastasis. The lymphangiostatic features of 16K hPRL might also be related to tissue remodeling, which accompanies the formation of new vessels (48). *In vivo* tissue remodeling is dependent on activation of urokinase type plasminogen activator, which is inhibited by activation of plasminogen activator inhibitor (PAI-1). PAI-1 is up-regulated by 16K hPRL, which is in line with our hypothesis (1, 3). However, recently Bruyere *et al.* (49) demonstrated that PAI-1 deficiency did not affect tumor lymphangiogenesis. This also suggests that vascular remodeling associated with lymphangiogenesis and angiogenesis might involve different molecular determinants.

In contrast to our earlier work in which we demonstrated that 16K hPRL significantly prevents hematogenic B16F10 tumor metastasis (19), here we were unable to observe a clear impact of 16K-Ad treatment in the lymphogenic metastasis model. The eGFP-B16F10 footpad model has been described in the literature as a spontaneous metastasis model, with metastatic lesions in the sentinel lymph node derived from the primary tumor in the footpad (32–34). When we scrutinized the metastatic dissemination in this footpad model, we observed already after 48 h after tumor inoculation into the footpad the presence of B16F10 melanoma cells in the SLN; this was before the development of a primary tumor. These results are not in agreement with a spontaneous metastasis model in which tumor cells disseminate from the primary tumor, and the results obtained cannot be interpreted as such. The footpad contains a lymphatic-vascular network and consequently our hypothesis is that tumor cells injected into the footpad have direct access to the lymphatic system. For that reason, due to the fast tumor cell dissemination, we speculate that the eGFP-B16F10 footpad tumor model seems to be an experimental metastasis mouse model in which tumor cells are injected directly in the vasculature to mimic the development of metastatic lesions. Similar to the experimental lung metastasis B16F10 melanoma model of Nguyen *et al.* (19), we tried to determine the number of metastatic lesions per SLN and their sizes. Un-

fortunately, we were unable to accurately quantify these properties of the tiny tissues.

Recently two angiogenesis laboratories presented independently intriguing evidence that VEGF-targeted drugs inhibiting primary tumor growth might still shorten the survival of mice by promoting tumor metastasis (50, 51). This sheds new light on the angiostatic treatment of cancer, and all new angiostatic compounds should therefore be handled with caution. Thus, it is important that the effect of 16K hPRL is tested in well-characterized spontaneous metastasis models in the near future before the initiation of clinical trials.

In conclusion, we demonstrated that 16K hPRL is a potent angiostatic agent with additional lymphangiostatic properties, providing it with the potential for use in anticancer therapies.

Acknowledgments

We acknowledge the GIGA Research mouse facility (Pierre Drion).

Address all correspondence and requests for reprints to: Ingrid Struman, GIGA Research, Molecular Biology and Genetic Engineering Unit, University of Liège, 4000 Liège, Belgium. E-mail: i.struman@ulg.ac.be.

This work was supported by grants from the Fonds pour la Recherche Industrielle et Agricole, the Fonds National de la Recherché Scientifique, the Grant FP7-HEALTH-2007-A, Proposal 201279 "MICROENVIMET," and the Neoangio Program of the Walloon Region.

Disclosure Summary: No author has anything to disclose.

References

1. **Lee H, Struman I, Clapp C, Martial J, Weiner RI** 1998 Inhibition of urokinase activity by the antiangiogenic factor 16K prolactin: activation of plasminogen activator inhibitor 1 expression. Endocrinology 139:3696–3703
2. **Martini JF, Piot C, Humeau LM, Struman I, Martial JA, Weiner RI** 2000 The antiangiogenic factor 16K PRL induces programmed cell death in endothelial cells by caspase activation. Mol Endocrinol 14:1536–1549
3. **Struman I, Bentzien F, Lee H, Mainfroid V, D'Angelo G, Goffin V, Weiner RI, Martial JA** 1999 Opposing actions of intact and N-terminal fragments of the human prolactin/growth hormone family members on angiogenesis: an efficient mechanism for the regulation of angiogenesis. Proc Natl Acad Sci USA 96:1246–1251
4. **Tabruyn SP, Nguyen NQ, Cornet AM, Martial JA, Struman I** 2005 The antiangiogenic factor, 16-kDa human prolactin, induces endothelial cell cycle arrest by acting at both the G0–G1 and the G2-M phases. Mol Endocrinol 19:1932–1942
5. **Tabruyn SP, Sorlet CM, Rentier-Delrue F, Bours V, Weiner RI, Martial JA, Struman I** 2003 The antiangiogenic factor 16K human prolactin induces caspase-dependent apoptosis by a mechanism that requires activation of nuclear factor-κB. Mol Endocrinol 17:1815–1823
6. **Piwnica D, Fernandez I, Binart N, Touraine P, Kelly PA, Goffin V** 2006 A new mechanism for prolactin processing into 16K PRL by secreted cathepsin D. Mol Endocrinol 20:3263–3278
7. **D'Angelo G, Martini JF, Iiri T, Fantl WJ, Martial J, Weiner RI** 1999 16K human prolactin inhibits vascular endothelial growth factor-induced activation of Ras in capillary endothelial cells. Mol Endocrinol 13:692–704
8. **D'Angelo G, Struman I, Martial J, Weiner RI** 1995 Activation of mitogen-activated protein kinases by vascular endothelial growth factor and basic fibroblast growth factor in capillary endothelial cells is inhibited by the antiangiogenic factor 16-kDa N-terminal fragment of prolactin. Proc Natl Acad Sci USA 92:6374–6378
9. **Ferrara N, Clapp C, Weiner R** 1991 The 16K fragment of prolactin specifically inhibits basal or fibroblast growth factor stimulated growth of capillary endothelial cells. Endocrinology 129:896–900
10. **Lee SH, Kunz J, Lin SH, Yu-Lee LY** 2007 16-kDa prolactin inhibits endothelial cell migration by down-regulating the Ras-Tiam1-Rac1-Pak1 signaling pathway. Cancer Res 67:11045–11053
11. **Clapp C, Weiner RI** 1992 A specific, high affinity, saturable binding site for the 16-kilodalton fragment of prolactin on capillary endothelial cells. Endocrinology 130:1380–1386
12. **Hilfiker-Kleiner D, Kaminski K, Podewski E, Bonda T, Schaefer A, Sliwa K, Forster O, Quint A, Landmesser U, Doerries C, Luchtefeld M, Poli V, Schneider MD, Balligand JL, Desjardins F, Ansari A, Struman I, Nguyen NQ, Zschemisch NH, Klein G, Heusch G, Schulz R, Hilfiker A, Drexler H** 2007 A cathepsin D-cleaved 16 kDa form of prolactin mediates postpartum cardiomyopathy. Cell 128:589–600
13. **González C, Parra A, Ramírez-Peredo J, García C, Rivera JC, Macotela Y, Aranda J, Lemini M, Arias J, Ibargüengoitia F, de la Escalera GM, Clapp C** 2007 Elevated vasoinhibins may contribute to endothelial cell dysfunction and low birth weight in preeclampsia. Lab Invest 87:1009–1017
14. **Erdmann S, Ricken A, Merkwitz C, Struman I, Castino R, Hummitzsch K, Gaunitz F, Isidoro C, Martial J, Spanel-Borowski K** 2007 The expression of prolactin and its cathepsin D-mediated cleavage in the bovine corpus luteum vary with the estrous cycle. Am J Physiol Endocrinol Metab 293:E1365–E1377
15. **Carmeliet P, Jain RK** 2000 Angiogenesis in cancer and other diseases. Nature 407:249–257
16. **Bentzien F, Struman I, Martini JF, Martial J, Weiner R** 2001 Expression of the antiangiogenic factor 16K hPRL in human HCT116 colon cancer cells inhibits tumor growth in Rag1(−/−) mice. Cancer Res 61:7356–7362
17. **Kim J, Luo W, Chen DT, Earley K, Tunstead J, Yu-Lee LY, Lin SH** 2003 Antitumor activity of the 16-kDa prolactin fragment in prostate cancer. Cancer Res 63:386–393
18. **Kinet V, Nguyen NQ, Sabatel C, Blacher S, Noël A, Martial JA, Struman I** 2009 Antiangiogenic liposomal gene therapy with 16K human prolactin efficiently reduces tumor growth. Cancer Lett 284:222–228
19. **Nguyen NQ, Cornet A, Blacher S, Tabruyn SP, Foidart JM, Noël A, Martial JA, Struman I** 2007 Inhibition of tumor growth and metastasis establishment by adenovirus-mediated gene transfer delivery of the antiangiogenic factor 16K hPRL. Mol Ther 15:2094–2100
20. **Cueni LN, Detmar M** 2008 The lymphatic system in health and disease. Lymphat Res Biol 6:109–122
21. **Swartz MA, Skobe M** 2001 Lymphatic function, lymphangiogenesis, and cancer metastasis. Microsc Res Tech 55:92–99
22. **Van Trappen PO, Pepper MS** 2002 Lymphatic dissemination of tumour cells and the formation of micrometastases. Lancet Oncol 3:44–52
23. **Hirakawa S** 2009 From tumor lymphangiogenesis to lymphvascular niche. Cancer Sci 100:983–989

24. **Sleeman JP, Thiele W** 2009 Tumor metastasis and the lymphatic vasculature. Int J Cancer 125:2747–2756
25. **Chambers AF, Groom AC, MacDonald IC** 2002 Dissemination and growth of cancer cells in metastatic sites. Nat Rev Cancer 2:563–572
26. **Stacker SA, Achen MG, Jussila L, Baldwin ME, Alitalo K** 2002 Lymphangiogenesis and cancer metastasis. Nat Rev Cancer 2:573–583
27. **Pan H, Nguyen NQ, Yoshida H, Bentzien F, Shaw LC, Rentier-Delrue F, Martial JA, Weiner R, Struman I, Grant MB** 2004 Molecular targeting of antiangiogenic factor 16K hPRL inhibits oxygen-induced retinopathy in mice. Invest Ophthalmol Vis Sci 45:2413–2419
28. **Deroanne CF, Colige AC, Nusgens BV, Lapiere CM** 1996 Modulation of expression and assembly of vinculin during *in vitro* fibrillar collagen-induced angiogenesis and its reversal. Exp Cell Res 224: 215–223
29. **Dunworth WP, Fritz-Six KL, Caron KM** 2008 Adrenomedullin stabilizes the lymphatic endothelial barrier *in vitro* and *in vivo*. Peptides 29:2243–2249
30. **Mikhaylova M, Mori N, Wildes FB, Walczak P, Gimi B, Bhujwalla ZM** 2008 Hypoxia increases breast cancer cell-induced lymphatic endothelial cell migration. Neoplasia 10:380–389
31. **Liang CC, Park AY, Guan JL** 2007 *In vitro* scratch assay: a convenient and inexpensive method for analysis of cell migration *in vitro*. Nat Protoc 2:329–333
32. **Harrell MI, Iritani BM, Ruddell A** 2007 Tumor-induced sentinel lymph node lymphangiogenesis and increased lymph flow precede melanoma metastasis. Am J Pathol 170:774–786
33. **Kawada K, Sonoshita M, Sakashita H, Takabayashi A, Yamaoka Y, Manabe T, Inaba K, Minato N, Oshima M, Taketo MM** 2004 Pivotal role of CXCR3 in melanoma cell metastasis to lymph nodes. Cancer Res 64:4010–4017
34. **Wiley HE, Gonzalez EB, Maki W, Wu MT, Hwang ST** 2001 Expression of CC chemokine receptor-7 and regional lymph node metastasis of B16 murine melanoma. J Natl Cancer Inst 93:1638–1643
35. **Clapp C, Martial JA, Guzman RC, Rentier-Delure F, Weiner RI** 1993 The 16-kilodalton N-terminal fragment of human prolactin is a potent inhibitor of angiogenesis. Endocrinology 133:1292–1299
36. **Matsui J, Funahashi Y, Uenaka T, Watanabe T, Tsuruoka A, Asada M** 2008 Multi-kinase inhibitor E7080 suppresses lymph node and lung metastases of human mammary breast tumor MDA-MB-231 via inhibition of vascular endothelial growth factor-receptor (VEGF-R) 2 and VEGF-R3 kinase. Clin Cancer Res 14:5459–5465
37. **Sini P, Samarzija I, Baffert F, Littlewood-Evans A, Schnell C, Theuer A, Christian S, Boos A, Hess-Stumpp H, Foekens JA, Setyono-Han B, Wood J, Hynes NE** 2008 Inhibition of multiple vascular endothelial growth factor receptors (VEGFR) blocks lymph node metastases but inhibition of VEGFR-2 is sufficient to sensitize tumor cells to platinum-based chemotherapeutics. Cancer Res 68:1581–1592
38. **Schomber T, Zumsteg A, Strittmatter K, Crnic I, Antoniadis H, Littlewood-Evans A, Wood J, Christofori G** 2009 Differential effects of the vascular endothelial growth factor receptor inhibitor PTK787/ZK222584 on tumor angiogenesis and tumor lymphangiogenesis. Mol Cancer Ther 8:55–63
39. **Brideau G, Mäkinen MJ, Elamaa H, Tu H, Nilsson G, Alitalo K, Pihlajaniemi T, Heljasvaara R** 2007 Endostatin overexpression inhibits lymphangiogenesis and lymph node metastasis in mice. Cancer Res 67:11528–11535
40. **Fukumoto S, Morifuji M, Katakura Y, Ohishi M, Nakamura S** 2005 Endostatin inhibits lymph node metastasis by a down-regulation of the vascular endothelial growth factor C expression in tumor cells. Clin Exp Metastasis 22:31–38
41. **Heishi T, Hosaka T, Suzuki Y, Miyashita H, Oike Y, Takahashi T, Nakamura T, Arioka S, Mitsuda Y, Takakura T, Hojo K, Matsumoto M, Yamauchi C, Ohta H, Sonoda H, Sato Y** 2010 Endogenous angiogenesis inhibitor vasohibin1 exhibits broad-spectrum antilymphangiogenic activity and suppresses lymph node metastasis. Am J Pathol 176:1950–1958
42. **Shao XJ, Chi XY** 2005 Influence of angiostatin and thalidomide on lymphangiogenesis. Lymphology 38:146–155
43. **Hawighorst T, Oura H, Streit M, Janes L, Nguyen L, Brown LF, Oliver G, Jackson DG, Detmar M** 2002 Thrombospondin-1 selectively inhibits early-stage carcinogenesis and angiogenesis but not tumor lymphangiogenesis and lymphatic metastasis in transgenic mice. Oncogene 21:7945–7956
44. **Ichise T, Yoshida N, Ichise H** 2010 H-, N- and Kras cooperatively regulate lymphatic vessel growth by modulating VEGFR3 expression in lymphatic endothelial cells in mice. Development 137: 1003–1013
45. **Gonzalez C, Corbacho AM, Eiserich JP, Garcia C, Lopez-Barrera F, Morales-Tlalpan V, Barajas-Espinosa A, Diaz-Muñoz M, Rubio R, Lin SH, Martinez de la Escalera G, Clapp C** 2004 16K-prolactin inhibits activation of endothelial nitric oxide synthase, intracellular calcium mobilization, and endothelium-dependent vasorelaxation. Endocrinology 145:5714–5722
46. **Lee SH, Nishino M, Mazumdar T, Garcia GE, Galfione M, Lee FL, Lee CL, Liang A, Kim J, Feng L, Eissa NT, Lin SH, Yu-Lee LY** 2005 16-kDa prolactin down-regulates inducible nitric oxide synthase expression through inhibition of the signal transducer and activator of transcription 1/IFN regulatory factor-1 pathway. Cancer Res 65: 7984–7992
47. **Lahdenranta J, Hagendoorn J, Padera TP, Hoshida T, Nelson G, Kashiwagi S, Jain RK, Fukumura D** 2009 Endothelial nitric oxide synthase mediates lymphangiogenesis and lymphatic metastasis. Cancer Res 69:2801–2808
48. **Dass K, Ahmad A, Azmi AS, Sarkar SH, Sarkar FH** 2008 Evolving role of uPA/uPAR system in human cancers. Cancer Treat Rev 34: 122–136
49. **Bruyère F, Melen-Lamalle L, Blacher S, Detry B, Masset A, Lecomte J, Lambert V, Maillard C, Hoyer-Hansen G, Lund LR, Foidart JM, Noël A** 2010 Does plasminogen activator inhibitor-1 drive lymphangiogenesis? PLoS One 5:e9653
50. **Ebos JM, Lee CR, Cruz-Munoz W, Bjarnason GA, Christensen JG, Kerbel RS** 2009 Accelerated metastasis after short-term treatment with a potent inhibitor of tumor angiogenesis. Cancer Cell 15:232–239
51. **Pàez-Ribes M, Allen E, Hudock J, Takeda T, Okuyama H, Viñals F, Inoue M, Bergers G, Hanahan D, Casanovas O** 2009 Antiangiogenic therapy elicits malignant progression of tumors to increased local invasion and distant metastasis. Cancer Cell 15:220–231